Astron. Nachr. / AN **999**, No. 88, 789 – 793 (2006) / **DOI** ***please set DOI!***

Modelling the broad-band spectra of X-ray emitting GPS galaxies

L. Ostorero[1,2,⋆], **R. Moderski**[3], **Ł. Stawarz**[4,5], **M.C. Begelman**[6], **A. Diaferio**[1,2], **I. Kowalska**[7], **J. Kataoka**[8]**,** and **S.J. Wagner**[9]

[1] Dipartimento di Fisica Generale "Amedeo Avogadro", Università di Torino, Via P. Giuria 1, 10125 Torino, Italy
[2] Istituto Nazionale di Fisica Nucleare (INFN), Via P. Giuria 1, 10125 Torino, Italy
[3] Nicolaus Copernicus Astronomical Center, Bartycka 18, 00-716 Warsaw, Poland
[4] Kavli Institute for Particle Astrophysics and Cosmology, Stanford University, Stanford CA 94305
[5] Astronomical Observatory, Jagiellonian University, ul. Orla 171, 30-244 Kraków, Poland
[6] Joint Institute for Laboratory Astrophysics, University of Colorado, Boulder, CO 80309-0440, USA
[7] Astronomical Observatory, University of Warsaw, Al. Ujazdowskie 4, 00-478 Warsaw, Poland
[8] Department of Physics, Tokyo Institute of Technology, 2-12-1, Ohokayama, Meguro, Tokyo, 152-8551, Japan
[9] Landessternwarte Heidelberg-Königstuhl, Königstuhl 12, 69117 Heidelberg, Germany

The dates of receipt and acceptance should be inserted later

Key words galaxies: active – galaxies: nuclei – galaxies: jets – galaxies: ISM – radiation mechanism: non-thermal

The study of the broad-band emission of GHz-Peaked-Spectrum (GPS) radio galaxies is a powerful tool to investigate the physical processes taking place in the central, kpc-sized region of their active hosts, where the jets propagate and the lobes expand, interacting with the surrounding interstellar medium (ISM). We recently developed a new dynamical-radiative model to describe the evolution of the GPS phenomenon (Stawarz et al. 2008): as the relativistic jets propagate through the ISM, gradually engulfing narrow-line emitting gas clouds along their way, the electron population of the expanding lobes evolves, emitting synchrotron light, as well as inverse-Compton radiation via up-scattering of the photon fields from the host galaxy and its active nucleus. The model, which successfully reproduces the key features of the GPS radio sources as a class, provides a description of the evolution of their spectral energy distribution (SED) with the lobes' expansion, predicting significant and complex X-ray to γ-ray emission. We apply here the model to the broad-band SED's of a sample of known, X-ray emitting GPS galaxies, and show that: (i) the free-free absorption mechanism enables us to reproduce the radio continuum at frequencies below the turnover; (ii) the lobes' non-thermal, inverse-Compton emission can account for the observed X-ray spectra, providing a viable alternative to the thermal, accretion-dominated scenario. We also show that, in our sample, the relationship between the X-ray and radio hydrogen column densities, $N_{\rm H}$ and $N_{\rm HI}$, is suggestive of a positive correlation, which, if confirmed, would support the scenario of high-energy emitting lobes.

1 Introduction

It is currently accepted that the GPS galaxies sample the youngest fraction of the population of powerful radio galaxies. From sub-kpc scales, their jet-lobe's structures propagate through the host-galaxy ISM, evolving into sub-galactic (Compact Steep Spectrum, CSS) sources, which then expand to super-galactic scales (see O'Dea 1998 for a review). However, this scenario still has several open issues, like the absorption mechanism responsible for the characteristic turnover in the radio spectrum, the details of the dynamical evolution and interaction with the ISM, the parameters of the central engine, and the origin of the high-energy emission. We recently proposed a model which addresses some of these issues through the analysis of the broad-band emission of GPS galaxies (Stawarz et al. 2008).

Here we show that our model appears to be promising, enabling us to reproduce a number of observed properties of a sample of X-ray emitting GPS galaxies.

⋆ Corresponding author: e-mail: ostorero@ph.unito.it

2 The model

We recall below the key features of our dynamical-radiative model, referring the reader to Stawarz et al. (2008), and references therein, for a more comprehensive discussion.

Our description of the dynamical evolution of GPS sources mounts on the model proposed by Begelman & Cioffi (1989) to explain the expansion of classical double sources in an ambient medium with density profile $\rho(r)$. The relevant equations can be derived by assuming that: (i) the jet momentum flux (proportional to the jet kinetic power $L_{\rm j}$) is balanced by the ram pressure of the ambient medium spread over an area $A_{\rm h}$, (ii) the lobes' sideways expansion velocity equals the speed of the shock driven by the overpressured cocoon, with internal pressure p, in the surrounding medium, and (iii) the energy $L_{\rm j}t$ transported by the jet pair during the source lifetime is converted into the cocoon's internal pressure. For young GPS sources with age t, linear size $LS(t) \lesssim 1$ kpc, and transverse size $l_{\rm c}(t)$, expanding in the central core of the gaseous halo of the elliptical host galaxy, we could constrain the model with a number of reasonable assumptions: (i) a constant ambient density $\rho = m_p n_0$ (with m_p the proton mass, and $n_0 \simeq 0.1$ cm^{-3}), representative of the King-profile's core, (ii) a constant hot-spot advance velocity $v_{\rm h} \simeq 0.1c$, as suggested by many observations of compact symmetric objects (but see Kawakatu, Nagai, & Kino 2009 for alternative scenarios), (iii) a scaling law $l_{\rm c}(t) \sim t^{1/2}$, reproducing the initial, ballistic phase of the jet propagation. All the lobes' physical quantities become thus functions of two parameters only: the jet kinetic power $L_{\rm j}$ and the source linear size LS.

We then studied how the broad-band radiative output of GPS sources evolves as the source expands, for a given jet power $L_{\rm j}$. The magnetic field in the expanding lobes scales as $B = (8\pi\eta_B p)^{1/2} \sim L_{\rm j}^{1/4} LS^{-1/2}$, with $\eta_B = U_B/p < 3$, and U_B the magnetic energy density. The electron population $Q(\gamma)$ (with γ the electron's Lorentz factor), injected from the terminal jet shocks to the expanding lobes, evolves under the joint action of adiabatic and radiative energy losses, yielding a lobes' electron population $N_e(\gamma)$, which has a broken power-law form with critical energy $\gamma_{\rm cr}$ when $Q(\gamma)$ is a power law, and a more complex form when $Q(\gamma)$ is a broken power law with intrinsical break $\gamma_{\rm int} \simeq 2\,10^3$. Assuming that the lobes' electrons, in rough equipartition with the magnetic field and the cold protons, provide the bulk of the lobes' pressure, the electron energy density is $U_e = \eta_e p$, with $\eta_e \lesssim 3$. The lobes'electrons are source of synchrotron radiation, with luminosity $L_{\rm syn}$ constant with time, and energy density $U_{\rm syn} \sim LS^{-3/2}$. Free-free absorption (FFA) of this radiation by neutral-hydrogen clouds of the narrow-line region (NLR), engulfed by the expanding lobes and photoionized on their surface by the radiation from the active nucleus (as proposed by Begelman 1999), is the process which we favour for the formation of the inverted spectra. While the synchrotron-self-absorption (SSA) process does not enable us to reproduce the observed turnover frequencies $\nu_{\rm p}$, the spectra below the turnover, and the $\nu_{\rm p} - LS$ anticorrelation (O'Dea & Baum 1997), FFA effects best fit the inverted spectra, and are a promising candidate to account for the above anticorrelation.

The lobes' particles also produce inverse-Compton (IC) radiation via up-scattering of both the synchrotron radiation (synchrotron-self-Compton mechanism; SSC) and the local, thermal photon fields generated by the accretion disc, the torus, and the stellar population of the host galaxy. The energy density $U_{\rm rad}$ of the thermal fields was evaluated by assuming that the nuclei of GPS sources share the properties of quasars and Seyfert galaxies. The accretion disc, assumed to produce the bulk of its luminosity (10^{45-47}erg s^{-1} ; e.g., Koratkar & Blaes 1999) at UV frequencies, provides $U_{\rm UV} \sim LS^{-2}$; the dusty torus, radiating the disc's UV photons at IR frequencies with efficiency $\epsilon \sim 10 - 100\%$, yields $U_{\rm IR} \sim LS^{-2}$; finally, the host galaxy contributes near-IR to optical photons with $U_{\rm opt}$ independent of LS. The IC scattering of all the above radiation fields yields significant and complex high-energy emission, from X-ray to γ-ray energies. Whereas in GPS *quasars* the direct X-ray emission of the accretion disc's hot corona and of the beamed relativistic jets may overcome the X-ray output of most of these sources, in GPS *galaxies* those contributions are expected to be obscured by the torus and Doppler-hidden, respectively, and the lobes are expected to be the dominant X-ray source.

3 Observational supports

Our model, and specifically the prediction of the X-ray–emitting lobes, may be supported by further observational evidence, which we did not discuss in Stawarz et al. (2008).

The X-ray emission of GPS galaxies has been traditionally interpreted as thermal radiation from the accretion disc, absorbed by a gas component associated with the AGN and characterized by an equivalent hydrogen column density $N_{\rm H}$ (O'Dea et al. 2000; Guainazzi et al. 2004, 2006; Vink et al. 2006; Siemiginowska et al. 2008), rather than as non-thermal emission from the jets or the lobes. The former scenario is mainly based on the apparent discrepancy between the equivalent total-hydrogen column density $N_{\rm H}$ derived from the X-ray spectral analysis and the neutral-hydrogen column density $N_{\rm HI}$ derived from the 21-cm radio measurements. Because $N_{\rm H}$ always appeared to exceed $N_{\rm HI}$ of 1–2 orders of magnitudes, it came natural to interpret the X-rays as produced in a source region which is more obscured than the region where the bulk of the radio emission comes from, and thus located *in between* the radio lobes; otherwise, an unreasonably high fraction of ionized hydrogen (H II) would be necessary to account for the above difference (e.g., Guainazzi et al. 2006; Vink et al. 2006). Such a scenario would also be consistent with the observed anticorrelation between $N_{\rm HI}$ and linear size found by Pihlström, Conway & Vermeulen (2003), being the fraction of ionized gas likely low in a young radio source with still expanding Strömgren sphere (Vink et al. 2006).

The discrepancies between the $N_{\rm H}$ and $N_{\rm HI}$ values mentioned above should actually be regarded with caution. The $N_{\rm HI}$ estimate is derived, from the measurements of the H I absorption lines, as a function of the ratio between the spin temperature $T_{\rm s}$ of the gas and its covering factor $c_{\rm f}$, representing the fraction of the source covered by the H I screen (e.g., Gupta et al. 2006). The common assumption $T_{\rm s}/c_{\rm f} = 100$ K refers to the case of complete coverage ($c_{\rm f} = 1$) of the emitting source by a standard cold ($T_{\rm k} \simeq 100$ K) ISM cloud in thermal equilibrium, and thus with spin temperature equal to the kinetic temperature ($T_{\rm s} = T_{\rm k}$). However, this assumption returns a value of $N_{\rm HI}$ which represents a lower limit to the actual neutral hydrogen column density (Pihlström et al. 2003; Vermeulen et al. 2003; Gupta et al. 2006). In fact, in the AGN environment, illumination by X-ray radiation might easily raise $T_{\rm k}$ up to $10^3 - 10^4$ K (Conway & Blanco 1995; Maloney, Hollenbach, & Tielens 1996), making $T_{\rm s}$ raise accordingly (Davies & Cummings 1975; Liszt 2001); a source covering factor smaller than unity would also increase the $T_{\rm s}/c_{\rm f}$ ratio. Both the above effects might lead to $N_{\rm HI}$ values fully consistent with the

N_H estimates. Finally, temperatures as high as several 10^3 K would likely imply the presence of a non-negligible fraction of H II (Maloney et al. 1996; Vink et al. 2006), also contributing to relax possible residual column-density discrepancies. The consistency of N_H and N_{HI} would make the scenario of non-thermal X-ray–emitting lobes a viable alternative to the accretion-disc dominated model.

Evidence is mounting that, in GPS and CSS sources, the H I absorption lines are not generated by a screen covering the source uniformly: instead, they seem to originate in clouds of neutral hydrogen connected with the radio structures of their jets and/or lobes, and possibly interacting with them (Morganti et al. 2004; Labiano et al. 2006; Vermeulen et al. 2006). The association of the bulk of the H I absorption with the optical emission lines currently supports the identification of the absorbers with the atomic cores of the NLR clouds, although the presence of H I elsewhere is not ruled out (Labiano et al. 2006; Vermeulen et al. 2006).

In our GPS model, the NLR clouds are gradually engulfed by the expanding lobes: besides being responsible for the FFA of the radio photons, they might play an important role in the absorption of the lobes' X-ray radiation.

4 Comparison with broad-band data

4.1 Modelling the SED's

We tested our dynamical-radiative model on the 11 GPS galaxies currently known as X-ray emitters.[1] In Fig. 1, we show, as an example, the modelling of the intrinsic[2] broad-band SED of B0108+388, a source with $LS = 41$ pc. The SED data were derived from the literature, and properly de-absorbed. The modelling of the complete SED sample will be presented elsewhere.

The radio data of IERS B0108+388 were modelled as synchrotron radiation produced by a lobes' electron population $N_e(\gamma)$ derived from the evolution of an injected hot-spots' population $Q(\gamma) \sim \gamma^{-s}$, with $s = s_1 = 1.8$ for $\gamma < \gamma_{\rm int}$, and $s = s_2 = 3.2$ for $\gamma > \gamma_{\rm int}$. FFA effects enable us to best fit the spectral behaviour at frequencies below the $\simeq 6$ GHz turnover. The thermal emissions from the torus (IR), the disc (UV), and the host galaxy (optical-NIR) were modelled as black-body spectra with the appropriate frequency peaks ($\nu_{\rm IR} = 0.5\,10^{13}$ Hz, $\nu_{\rm UV} = 2.45\,10^{15}$ Hz, and $\nu_{\rm opt} = 2.0\,10^{14}$ Hz) and bolometric luminosities ($L_{\rm IR} = 5.0\,10^{44}$ erg s^{-1}, $L_{\rm UV} = 5.0\,10^{45}$ erg s^{-1}, and $L_{\rm opt} = 6.0\,10^{44}$ erg s^{-1}). The comptonization of the synchrotron and thermal radiation fields yields the high-energy spectral components. For this source, the X-ray emission is dominated by the comptonization of the IR radiation. Our model well reproduces the observed X-ray spectrum, and predicts significant γ-ray emission.

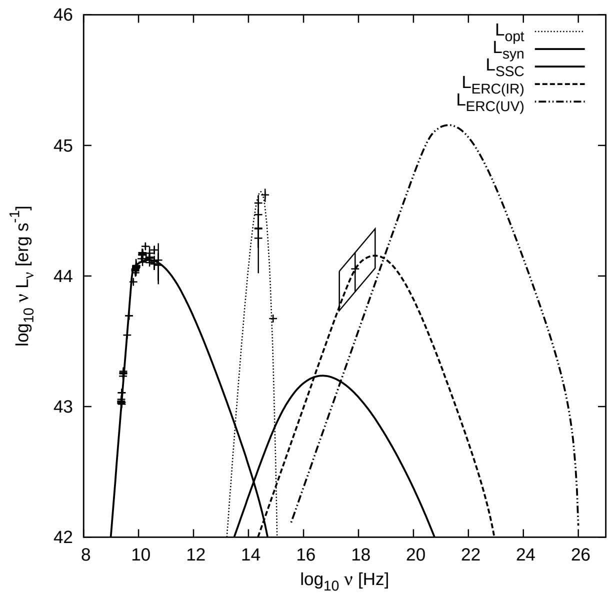

Fig. 1 Modelling of the intrinsic SED of GPS galaxy IERS B0108+388. Radio to X-ray data were derived from: NED; Dallacasa et al. (2000); Tinti et al. (2005); Stickel et al. (1996); Vink et al. (2006). The curves show the modelled spectral components: synchrotron emission, and corresponding SSC emission (solid lines); thermal star light (dotted line); comptonized thermal emission from the torus and the disc, respectively (dashed and dash-dot-dotted lines). The comptonized starlight's luminosity does not appear in the plot because it is lower than 10^{42} erg s^{-1}.

4.2 N_H -N_{HI} connection

Besides the modelling of the broad-band SED's, a way of discriminating among different scenarios, and unveil the actual X-ray production site, is to compare the properties of the X-ray and radio absorbers, i.e. the N_H and N_{HI} column densities. Such a comparison can be performed either for individual sources, where an *ad hoc* increase of the T_s parameter can remove possible N_H and N_{HI} discrepancies, or for a source sample, where the existence of a positive, significant N_H -N_{HI} correlation would suggest that the X-ray and radio absorbers coincide, thus supporting the co-spatiality of the X-ray and radio source.

We investigated the existence of a connection between N_H and N_{HI} in our sample. For a positive correlation, we searched the source subsample for which both N_H and N_{HI} estimates (either detections or upper limits) are available (see Fig. 2, and footnote 1). We obtained the following results: (1) the subsample of 5 sources for which both N_H and N_{HI} *detections* are available displays a strong (Pearson's

[1] IERS B0026+346, IERS B0108+388⋆, IERS B0500+019⋆, IERS B0710+439, PKS B0941-080, IERS B1031+567⋆, IERS B1345+125⋆, IVS B1358+624⋆, IERS B1404+286, IERS B2128+048, IERS B2352+495⋆. Sources marked with an asterisk are those of the subsample discussed in Sec. 4.2, and included in Fig. 2.

[2] Throughout this paper, we use the cosmological paramters: $\Omega_\Lambda = 0.7$, $\Omega_M = 0.3$, with $H_0 = 72$ km s^{-1} Mpc^{-1}

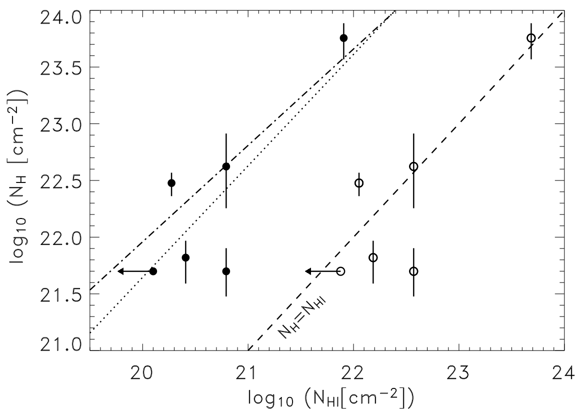

Fig. 2 N_H vs. N_{HI} for 6 GPS's of our sample[1]. Solid symbols: N_{HI} was computed with $T_s = 100$ K; arrows are upper limits. Open symbols: as an example, the same sources with $T_s = 6\,10^3$ K are shown. Dash-dotted line: linear fit to the 5-source subsample of N_H /N_{HI} *detections* (with $T_s = 100$ K); dotted line: linear fit to the 6-source subsample including both *detections* and *upper limits*; Data are from: Guainazzi et al. (2006); Mirabel (1989); O'Dea et al. (2000); Pihlström et al. (2003); Siemiginowska et al. (2008); Vermeulen et al. (2003); Vink et al. (2006).

$r = 0.997$) and highly significant ($S = 2.3 \cdot 10^{-4}$) N_H - N_{HI} positive correlation; (2) in the above-mentioned subsample, the strength and significance of the correlation substantially decrease when using non-parametric methods (Kendall's and Spearman's correlation coefficients; e.g., Press et al. 1992); (3) the 6-source subsample including the N_{HI} *upper limit* also shows, according to survival analysis techniques (ASURV, Rev. 1.2; e.g., La Valley, Isobe & Feigelson 1992), a positive correlation, however with lower strength ($\rho \sim 0.6$), and a significance varying in the range $S = 0.17 - 0.33$, depending on both the N_H value (when more than one is available) and the statistical method chosen for the analysis. Although the data are suggestive of a positive correlation, further measurements would definitely help to improve the statistics.

5 Conclusions and future prospects

Our dynamical-radiative model can reproduce the observed broad-band SED's of X-ray emitting GPS galaxies. The shape of the radio spectra at frequencies below the turnover is best fitted by assuming FFA effects as the dominant absorption mechanism, whereas the X-ray spectra can be ascribed to IC scattering of the thermal radiation fields (accretion disc, torus, and host galaxy) off the lobes' electron population. Further observational support to the X-ray–lobes' scenario comes from the radio and X-ray hydrogen column densities of a sample of X-ray GPS's: the data suggest a positive correlation, which, if confirmed, would point towards the co-spatiality of the radio and X-ray emission sites. Additional measurements, necessary to improve the statistics, are already planned.

Acknowledgements. This research has made use of the NASA/IPAC Extragalactic Database (NED), which is operated by the JPL, Caltech, under contract with the NASA. L.O. and A.D. acknowledge partial support from the INFN grant PD51. Ł.S., R.M., J.K., and S.W. acknowledge support by MEiN grant 1-P03D-003-29, MNiSW grant N N203 301635, JSPS KAKENHI (19204017/14GS0211), and BMBF/DLR grant 50OR0303, respectively. This work has benefited from research funding from the European Community's sixth Framework Programme under RadioNet R113CT 2003 5058187. We are indebted with L. Costamante, A. Siemiginowska, M. Guainazzi, R. Morganti, and E. Ferrero for helpful discussions on GPS's. L.O. and Ł.S. are grateful to M.J. Geller and A. Siemiginowska for their kind hospitality at the CfA. We thank the referees for their relevant and appropriate comments.

References

Begelman, M.C., Cioffi, D.F.: 1989, ApJ 345, L21
Begelman, M.C.: 1999, in The Most Distant Radio Galaxies, eds. H.J.A. Röttgering, P.N. Best, M.D. Lehnert (Amsterdam Royal Netherlands Acad. Arts and Sciences), 173
Conway, J.E., Blanco, P.R.: 1995, ApJ 449, L131
Dallacasa, D., Stanghellini, C., Centonza, M., Fanti, R.: 2000, A&A 363, 887
Davies, R.D. Cummings. E.R.: 1975, MNRAS 170, 95
Guainazzi, M., Siemiginowska, A., Rodriguez-Pascual, P., Stanghellini, C.: 2004, A&A 421, 461
Guainazzi, M., Siemiginowska, A., Stanghellini, C., Grandi, P., Piconcelli, E., Azubike Ugwoke, C.: 2006, A&A 446, 87
Kawakatu, N., Nagai, H., Kino, M.: 2009, AN 330, this issue
Koratkar, A., Blaes, O.: 1999, PASP 111, 1
Labiano, A., Vermeulen, R.C., Barthel, P.D., O'Dea, C.P., Gallimore, J.F., Baum, S., de Vries, W.: 2006, A&A 447, 481
La Valley, M.P., Isobe, T., Feigelson, E.D.: 1992, BAAS 24, 839
Listz, H.: 2001, A&A 371, 698
Maloney, P.R., Hollenbach, D., Tielens, A.G.G.M.: 1996, ApJ 466, 561
Mirabel, I.F.: 1989, ApJ 340, L13
Morganti, R., Oosterloo, T.A., Tadhunter, C.N., Vermeulen, R., Pihlström, Y.M., van Moorsel, G., Wills, K.A.: 2004, A&A 424, 119
O'Dea, C.P.: 1998, PASP 110, 493
O'Dea, C.P., Baum, S.A.: 1997, AJ 113, 148
O'Dea, C.P., de Vries, W.H., Worrall, D.M., Baum, S., Koekemoer, A.: 2000, AJ 119, 478
Pihlström, Y.M., Conway, J.E., Vermeulen, R.C.: 2003, A&A 404, 871
Press, W.H., Teukolski, S.A., Vettering, W.T., Flannery, B.: 1992, Numerical recipes in FORTRAN - The art of scientific computing, Cambridge: University Press, 2nd ed.
Siemiginowska, A., La Massa, S., Aldcroft, T., Bechtold, J., Elvis, M.: 2008, ApJ 684, 811
Stawarz, Ł., Ostorero, L., Begelman, M.C., Moderski, R., Kataoka, J., Wagner, S.: 2008, ApJ 680, 911
Stickel, M., Rieke, G.H., Kühr, H., Rieke, M.J.: 1996, ApJ 468, 556
Tinti, S., Dallacasa, D., de Zotti, G., Celotti, A., Stanghellini, C.: 2005, A&A 432, 31
Vermeulen, R.C., Pihlström, Y.M., Tschager, W., et al.: 2003, A&A 404, 861

Vermeulen, R.C., Labiano, A., Barthel, P.D., Baum, S.A., de Vries, W.H., O'Dea, C.P.: 2006, A&A 447, 489
Vink, J., Snellen, I., Mack, K.-H., Schilizzi, R.: 2006, MNRAS 367, 928